Influence of antenna array constellation on the accuracy of angle-of-arrival estimation in a multipath environment

Thomas Lindner*, Niels Hadaschik**, Lucila Patiño-Studencka*, Jörn Thielecke*

*Friedrich-Alexander-Universität Erlangen-Nürnberg (FAU),
Institute of Information Technology (Communication Electronics), Am Wolfsmantel 33, 91058 Erlangen, Germany
**Fraunhofer Institute for Integrated Circuits (IIS), Nordostpark 93, 90411 Nürnberg, Germany

***Abstract*—Angle-of-arrival estimation is a widely used localization method. However, multipath propagation leads to decreased performance. In this paper an expression for the Cramer-Rao lower bound for angle-of-arrival estimation with a known transmitted signal in a two path environment is derived. The influence of array structure on the achievable accuracy and the capability of signal separation is investigated. It is shown that sparse array structures provide a lower Cramer-Rao bound as long as uniqueness is preserved.**

***Index Terms*—angle-of-arrival, array structure, multipath propagation, Cramer-Rao lower bound**

I. INTRODUCTION

The accuracy of angle estimation in a multipath (MP) environment is significantly degraded compared to the pure line of sight (LOS) scenario. In order to estimate the effect of a second propagation path the Cramer-Rao lower bound (CRLB) is used. The CRLB provides a best case bound for unbiased parameter estimation. An analytic expression, thus, gives insight regarding the parameters necessary for a accurate angle estimate and aids with optimizing those parameters which can be chosen while designing a localization system.

The CRLB for direction of arrival estimation has received much attention in the past [1]–[5]. In [4] a numerical evaluation for two signals impinging on a uniform linear array (ULA) is presented. In [5], Weiss et al. investigate the influence of correlation between sources with Gaussian distributed signals. Compared to the cited papers this paper focuses on the specific scenario, where the impinging signals are known and all signals are time shifted versions of the same signal (localization under multipath propagation). We contribute a simple perturbance term in the CRLB for the influence of the second path and compare different linear and uniform circular array geometries with regard to this CRLB.

Firstly in Section II we introduce the signal model used throughout this paper. Then Section III provides an analytic expression for the CRLB for angle estimation with two propagation paths, showing how the second path influences the first. The influence of the arising perturbance term is investigated for various antenna array constellations. The results are summarized in Section IV.

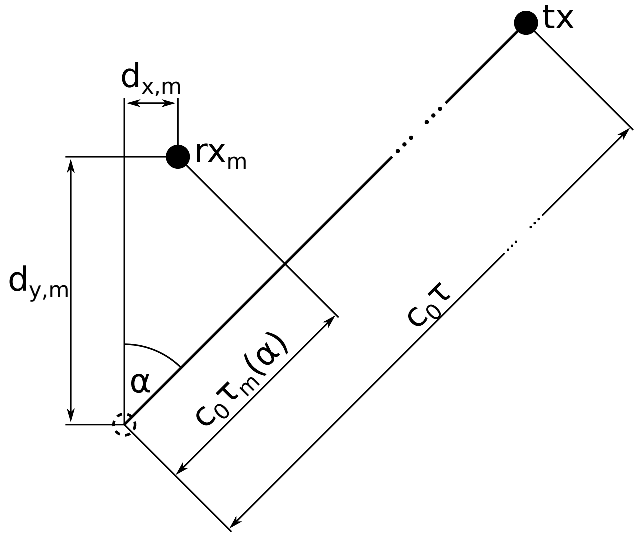

Fig. 1. Reception of a distant signal source tx by an array of closely spaced receiving elements rx_m. The element specific delay τ_m depends mostly on element position $(d_{x,m},\ d_{y,m})$ and angle of arrival α.

II. SIGNAL MODEL

The delay between a distant transmitter tx and a receiving element rx_m can be separated in a delay τ between the transmitter and the phase center of the array and an element-specific delay τ_m (see Figure 1). The element-specific delay is dependent on the distance of the phase center of the element relative to the phase center of the array $(d_{x,m},\ d_{y,m})$ and on the angle of arrival α of the incoming signal:

$$\tau_m(\alpha) = \frac{d_{x,m}\cos(\alpha) + d_{y,m}\sin(\alpha)}{c_0}\,. \tag{2.1}$$

So disregarding noise, the nth baseband sample at the mth antenna is

$$y_m[n] = \beta\exp(j2\pi f_c\tau_m(\alpha))s(nT - \tau + \tau_m(\alpha))\,, \tag{2.2}$$

where β is an unknown complex factor modeling the received signal amplitude and carrier phase, f_c is the carrier frequency

$$\mathrm{CRLB}^{-1} = \frac{2}{N_0} \begin{bmatrix} E_{s1}|\mathbf{a}'(\alpha_1)|^2 & \sqrt{E_{s1}E_{s2}}\,\mathrm{Re}\left(e^{j\Delta\varphi}\mathbf{a}'(\alpha_1)^{\mathrm{H}}\mathbf{a}'(\alpha_2)r(\Delta\tau)\right) \\ \sqrt{E_{s1}E_{s2}}\,\mathrm{Re}\left(e^{-j\Delta\varphi}\mathbf{a}'(\alpha_2)^{\mathrm{H}}\mathbf{a}'(\alpha_1)r(-\Delta\tau)\right) & E_{s2}|\mathbf{a}'(\alpha_2)|^2 \end{bmatrix} \tag{3.2}$$

$$\frac{1}{\mathrm{CRLB}_{\alpha_1}} = 2\frac{E_{s1}}{N_0}\left(|\mathbf{a}'(\alpha_1)|^2 - \underbrace{\frac{\mathrm{Re}\left(e^{j\Delta\varphi}\mathbf{a}'(\alpha_2)^{\mathrm{H}}\mathbf{a}'(\alpha_1)r(\Delta\tau)\right)^2}{|\mathbf{a}'(\alpha_2)|^2}}_{\text{perturbance term}}\right) \tag{3.3}$$

and $s(t)$ is the normalized complex envelope of the transmitted signal. This can be approximated as

$$y_m[n] \approx \beta\exp(j2\pi f_c\tau_m(\alpha))s(nT-\tau) \tag{2.3}$$

assuming that the bandwidth of $s(t)$ is low (narrowband assumption [6, p. 3]). Let us define two vectors, one depicting the phase change for the antennas (the steering vector) $\mathbf{a}(\alpha)$ and one depicting the received signal samples $\mathbf{s}(\tau)$:

$$\mathbf{a}(\alpha) = \begin{bmatrix}\exp(j2\pi f_c\tau_1(\alpha)) & \cdots & \exp(j2\pi f_c\tau_M(\alpha))\end{bmatrix}^{\mathrm{T}} \tag{2.4}$$

$$\mathbf{s}(\tau) = \begin{bmatrix}s(-\tau) & \cdots & s((N-1)T-\tau)\end{bmatrix}^{\mathrm{T}}. \tag{2.5}$$

We can write the matrix of received samples $\mathbf{Y}$ derived from (2.3) as

$$\begin{aligned}\mathbf{Y} &= \begin{bmatrix} y_1[0] & \cdots & y_1[N-1] \\ \vdots & & \vdots \\ y_M[0] & \cdots & y_M[N-1]\end{bmatrix} \\ &= \beta\mathbf{a}(\alpha)\mathbf{s}(\tau)^{\mathrm{T}}.\end{aligned} \tag{2.6}$$

For L paths and with additive white gaussian noise $\mathbf{W}$, we get

$$\begin{aligned}\mathbf{Y} &= \sum_{l=1}^{L}\beta_l\mathbf{a}(\alpha_l)\mathbf{s}(\tau_l)^{\mathrm{T}} + \mathbf{W} \\ &= \mathbf{A}(\boldsymbol{\alpha})\,\mathrm{diag}\,(\boldsymbol{\beta})\,\mathbf{S}(\boldsymbol{\tau})^{\mathrm{T}} + \mathbf{W},\end{aligned} \tag{2.7}$$

where $\mathbf{A}(\boldsymbol{\alpha})$ (the steering matrix) and $\mathbf{S}(\boldsymbol{\tau})$ are defined as

$$\mathbf{A}(\boldsymbol{\alpha}) = \begin{bmatrix}\mathbf{a}(\alpha_1) & \cdots & \mathbf{a}(\alpha_L)\end{bmatrix} \tag{2.8}$$

$$\mathbf{S}(\boldsymbol{\tau}) = \begin{bmatrix}\mathbf{s}(\tau_1) & \cdots & \mathbf{s}(\tau_L)\end{bmatrix}. \tag{2.9}$$

III. Cramer-Rao lower bound

In order to enable comparision, firstly, the bound for a single incident signal is given. It is easily derived (see appendix) as

$$\mathrm{CRLB}_\alpha = \frac{1}{2\frac{E_s}{N_0}|\mathbf{a}'(\alpha)|^2} \tag{3.1}$$

where E_s/N_0 is the energy to noise density ratio and $\mathbf{a}' = \frac{\partial\mathbf{a}}{\partial\alpha}$ is the derivative of the steering vector with regard to the angle of arrival. This CRLB for angle-of-arrival estimation is equivalent to the well known results in literature, e.g. [6, p. 37].

Considering the angle estimates for two paths arriving at the antenna array, we get the Fischer information matrix shown in (3.2), where $\Delta\varphi = \varphi_2 - \varphi_1$ is the difference in carrier phase between the first and the second path and $r(\Delta\tau)$ is the value of the normalized autocorrelation function of $s(t)$ at $\Delta\tau = \tau_2 - \tau_1$ (for the derivation see the appendix). Solving, the variance of the angle estimate for the first path (3.3) is obtained. It can be observed that this CRLB differs from the CRLB for a single path expressed in (3.1) by a perturbance term. The term vanishes, when the carrier phase difference $\Delta\varphi$ causes the product on the numerator of the perturbance term to have no real part. Since the difference in carrier phase between the paths cannot be controlled, we further assume the worst case, that is the difference $\Delta\varphi$ causes the product to contain no imaginary part. The perturbance term then simplifys to

$$\frac{|\mathbf{a}'(\alpha_2)^{\mathrm{H}}\mathbf{a}'(\alpha_1)r(\Delta\tau)|^2}{|\mathbf{a}'(\alpha_2)|^2}. \tag{3.4}$$

From (3.4) we can note that there are two factors influencing the perturbance term, namely the correlation between the paths $r(\Delta\tau)$ and the array specific scalar product $\mathbf{a}'(\alpha_2)^{\mathrm{H}}\mathbf{a}'(\alpha_1)$. Those two factors are analysed in the following sections. The influence of those parameters on the accuracy of the estimation for the the first angle α_1 depending on the angle separation $\Delta\alpha = \alpha_2 - \alpha_1$ is derived using some exemplary parameters.

A. Correlation between paths

Firstly the influence of the correlation between the paths $r(\Delta\tau)$ is analysed. In Figure 2a, the CRLB vs. angle difference between the paths for different correlation factors is depicted. A uniform linear array with $M = 4$ elements in half-wavelength spacing is assumed and the first path arrives at $\alpha_1 = 0\,°$ with $E_s/N_0 = 40\,\mathrm{dB}$.

For large differences in path length, the signals become approximately uncorrelated $r(\Delta\tau) \approx 0$, the perturbance term vanishes and the CRLB is independent from angle difference. If the difference in path lengths is small enougth, the signals become approximately fully correlated (coherent) $r(\Delta\tau) \approx 1$. In this case the CRLB becomes singular when $\alpha_1 = \alpha_2$ due to the non-identifiability of two signals. A real estimator would not detect two distinct signals in this case, let alone provide two unbiased estimates. For the correlation factors in-between, the CRLB gets worse with increasing values of r. The results confirm the general expectation that it is advantageous to use a signal with large bandwidth, achieving a narrow auto-correlation peak and, hence, low correlation factors for a given difference in path length.

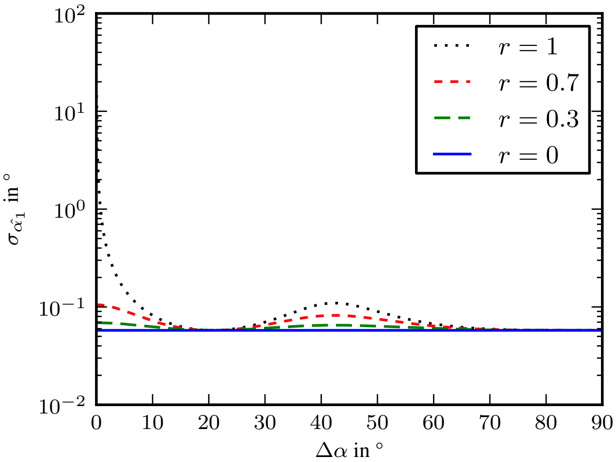

(a) Comparison of different correlation factors r. The array is a uniform linear array with $M = 4$ elements in half-wavelength spacing.

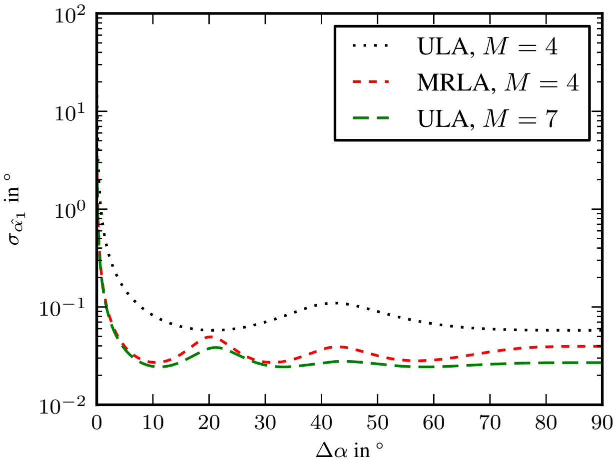

(b) Comparison of a minimum redundancy linear array (MRLA) with uniform linear arrays (ULA) of the same number of elements and same aperture respectively.

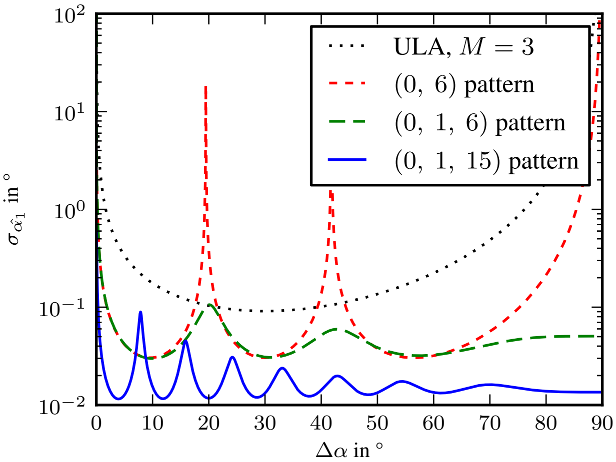

(c) Comparison of different sparse array patterns with the uniform linear array (ULA) of the same number of elements.

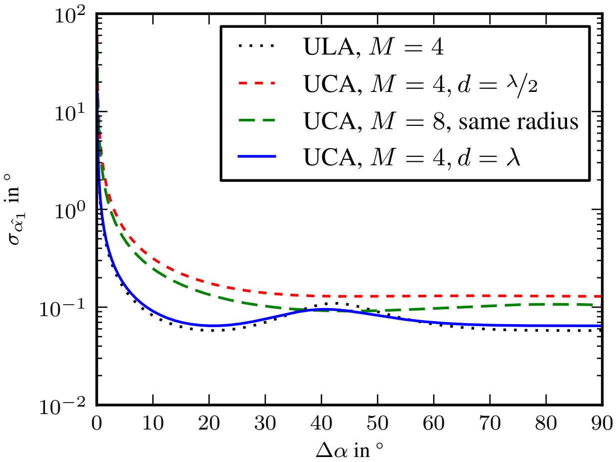

(d) Influence of the change of radius and element number on the CRLB of a uniform circular array (UCA) and comparison to a uniform linear array (ULA) of the same number of elements.

Fig. 2. CRLB for the first path vs. angle difference. For all graphs the first path is assumed to arrive at $\alpha_1 = 0\,°$ with $E_s/N_0 = 40\,\mathrm{dB}$.

B. Array structure

The other factor influencing the perturbance term is the array specific scalar product $\mathbf{a}'(\alpha_2)^{\mathrm{H}}\mathbf{a}'(\alpha_1)$. Analogous to the autocorrelation function being a measure for seperability in time this scalar product is a measure for seperability in the angle. The resulting bound is plotted vs. angle difference for different array structures in Figure 2b. As before the first path arrives at $\alpha_1 = 0\,°$ with $E_s/N_0 = 40\,\mathrm{dB}$. The paths are assumed to be fully correlated ($r = 1$).

Firstly linear arrays are considered. The dotted graph in Figure 2b depicts the CRLB for a four element array with uniform half-wavelength spacing (uniform linear array; ULA). We compared it to a non-uniform linear array with four elements at positions $(0,\ 1,\ 4,\ 6)$ (in units of half-wavelengths), so that each integer multiple of one half-wavelength occurs exactly once as spacing between two elements (minimum redundancy linear array; MRLA). The MRLA has a lower CRLB than the ULA with the same number of elements and achieves almost the CRLB for a ULA with the same aperture, which needs three elements more. This confirms that it is possible to outperform a ULA with a sparse pattern. However, a pattern with large element spacing can lead to ambiguity of the estimates, as shown next. The red short-dashed graph in Figure 2c shows the lower bound for two elements at positions $(0,\ 6)$. The singularity repeats at further angles, that cannot be distinguished from $0\,°$. In order to restore uniqueness, it is necessary to have at least one element spacing of one half-wavelength or less. Adding an element at position 1 restores uniqueness and leads to the green long-dashed graph. We observe that the requirement of each spacing between two elements occouring at least once is unnecessarily strict with respect to ambiguity resolution. It is possible to move the third element in a $(0,\ 1,\ x)$ configuration even further. Plotting the bound for a pattern of $(0,\ 1,\ 15)$ suggest increasing performance with larger apertures as expected. But note that increasing x too far violates the far-field assumptions.

In the following, circular arrays are considered. The red short-dashed graph in Figure 2d depicts the CRLB for a four element uniform circular array (UCA). The radius is chosen, so that the elements are one half-wavelength apart. Note that in our example the circular array performs worse than a linear arrays with the same number of elements shown as black dotted graph. This is because the signal arrives from an angle of $\alpha_1 = 0\,^\circ$, which is the best case for linear arrays. Doubling the number of elements, while keeping the radius the same, leads to the CRLB with the green long-dashed graph. The singularity becomes sharper implying a better resolution of close angles and the baseline for separate angles goes down as expected, when increasing the element number. If instead of increasing the number of elements the radius is increased, so that the spacing between the elements doubles, we get the bound shown with the blue solid graph. It can be seen that the circular array with large spacing achieves a bound compareable to that of the linear array with the same number of elements. Compared to linear arrays with large spacing the CRLB does not hint at ambiguity of the estimates. It is interesting to determine what radius is necessary to get the same baseline CRLB with a UCA as with a ULA assuming the same number of elements. Firstly note that the baseline CRLB is achieved when the perturbance term is zero. Therefore it is sufficient to compare (3.1) for the different array structures. The bounds differ only in the $|\mathbf{a}'(\alpha)|^2$ factor. It is well known in literature [6, p. 33/35], that

$$|\mathbf{a}'_{\mathrm{ULA}}(0)|^2 = \frac{\pi^2(M-1)M(M+1)}{12} \tag{3.5}$$

$$|\mathbf{a}'_{\mathrm{UCA}}(\alpha)|^2 = \frac{2\pi^2 r^2 M}{\lambda_c^2}\,, \tag{3.6}$$

where λ_c is the wavelength of the carrier frequency and r is the radius of the UCA. Therefore a UCA with

$$r = \lambda_c \sqrt{\frac{M^2-1}{24}} \tag{3.7}$$

achieves the same baseline CRLB as a ULA with the same number of elements.

IV. Conclusion

An expression for the CRLB of angle estimation in a two path channel has been derived. Comparison to the CRLB for a single path revealed a perturbance term. Further investigation of the perturbance term confirms that it is preferable to use a wideband signal with narrow auto-correlation peak and allows the exploration of different array structures. For linear arrays, it is shown that non-uniform structures achieve a lower CRLB even for two paths. It is not necessary that each integer multiple of one half-wavelength occours at least once as spacing between two elements, so wider apertures may be possible. For uniform circular arrays, doubling the radius leads to an even lower CRLB than doubling of elements, comparable to that of a linear array with the same number of elements. The CRLB does not show the repeating singularities, which hint at ambiguities in the case of linear arrays with increased element spacing. Further investigation gives an expression for the radius of the uniform circular array necessary to achieve the same baseline CRLB as a uniform linear array with the same number of elements. It would be interesting to verify to what extent this holds true for real circular arrays.

V. Acknowledgements

The work has been supported by EFRE funding from the Bavarian Ministry of Economic Affairs (Bayerisches Staatsministerium für Wirtschaft, Infrastruktur, Verkehr und Technologie) as a part of the ”ESI Application Center” project.

Appendix

In order to derive the CRLB, firstly, the signal model is vectorized resulting in

$$\begin{aligned} \mathbf{y} = \mathrm{vec}\left(\mathbf{Y}\right) &= \mathrm{vec}\left(\mathbf{A}(\boldsymbol{\alpha})\,\mathrm{diag}\left(\boldsymbol{\beta}\right)\mathbf{S}(\boldsymbol{\tau})^{\mathrm{T}}\right) + \mathbf{w} \\ &= \left(\mathbf{A}(\boldsymbol{\alpha}) \otimes \mathbf{S}(\boldsymbol{\tau})\right)\mathrm{vec}\left(\mathrm{diag}\left(\boldsymbol{\beta}\right)\right) + \mathbf{w} \\ &= \left(\mathbf{A}(\boldsymbol{\alpha}) \circ \mathbf{S}(\boldsymbol{\tau})\right)\boldsymbol{\beta} + \mathbf{w}\,, \end{aligned} \tag{A.1}$$

where $\otimes$ denotes the Kronecker product and $\circ$ denotes the Khatri-Rao product[1]. The noise vector $\mathbf{w}$ is circular symmetric complex normal distributed

$$\mathbf{w} = \mathrm{vec}\left(\mathbf{W}\right) \qquad \mathbf{w} \sim \mathcal{CN}\left(\mathbf{0}, N_0 B\,\mathbf{I}\right)\,. \tag{A.2}$$

It follows that the samples $\mathbf{y}$ are circular symmetric complex normal distributed

$$\mathbf{y} \sim \mathcal{CN}\,(\,\underbrace{\left(\mathbf{A}(\boldsymbol{\alpha}) \circ \mathbf{S}(\boldsymbol{\tau})\right)\boldsymbol{\beta}}_{\boldsymbol{\mu}_{\mathbf{y}}}, \underbrace{N_0 B\,\mathbf{I}}_{\boldsymbol{\Gamma}_{\mathbf{y}}}\,) \tag{A.3}$$

with mean $\boldsymbol{\mu}_{\mathbf{y}}$ and covariance $\boldsymbol{\Gamma}_{\mathbf{y}}$. The CRLB can be derived using a modification of the Slepian-Bangs formula for signals with circular symmetric complex normal distribution [7, p. 363] given as

$$\begin{aligned} [\mathrm{CRLB}^{-1}]_{ij} = \mathrm{tr}&\left(\boldsymbol{\Gamma}_{\mathbf{y}}{}^{-1}\frac{\partial\boldsymbol{\Gamma}_{\mathbf{y}}}{\partial\theta_i}\boldsymbol{\Gamma}_{\mathbf{y}}{}^{-1}\frac{\partial\boldsymbol{\Gamma}_{\mathbf{y}}}{\partial\theta_j}\right) \\ &+ 2\,\mathrm{Re}\left(\frac{\partial\boldsymbol{\mu}_{\mathbf{y}}}{\partial\theta_i}^{\mathrm{H}}\boldsymbol{\Gamma}_{\mathbf{y}}{}^{-1}\frac{\partial\boldsymbol{\mu}_{\mathbf{y}}}{\partial\theta_j}\right)\,, \end{aligned} \tag{A.4}$$

where θ_i are the estimated parameters. In our case the parameters of interest are

$$\boldsymbol{\theta} = \begin{bmatrix}\alpha_1 & \cdots & \alpha_L\end{bmatrix}^{\mathrm{T}}. \tag{A.5}$$

Taking the partial derivatives of (A.3) with respect to the parameters of interest, we obtain

$$\frac{\partial}{\partial\alpha_i}\boldsymbol{\Gamma}_{\mathbf{y}} = \mathbf{0} \qquad \frac{\partial}{\partial\alpha_i}\boldsymbol{\mu}_{\mathbf{y}} = \beta_i(\mathbf{a}'(\alpha_i) \otimes \mathbf{s}(\tau_i))\,, \tag{A.6}$$

where $\mathbf{a}' = \frac{\partial\mathbf{a}}{\partial\alpha}$ is the derivative of the steering vector with regard to the angle of arrival.

[1] columnwise Kronecker product

A. Single path ($L = 1$)

Considering only a single signal we have

$$\boldsymbol{\theta} = \begin{bmatrix}\alpha\end{bmatrix}^{\mathrm{T}} \tag{A.7}$$

and get

$$\mathrm{CRLB}^{-1} = 2\frac{|\beta|^2|\mathbf{a}'(\alpha)|^2|\mathbf{s}(\tau)|^2}{N_0 B}\,. \tag{A.8}$$

Using

$$|\beta|^2 = E_s \tag{A.9}$$

$$\begin{aligned}|\mathbf{s}(\tau)|^2 &= \sum_{n=0}^{N-1} |s(nT-\tau)|^2 \\ &\approx B\int_{-\infty}^{\infty} |s(t)|^2 \mathrm{d}t \\ &= B\end{aligned} \tag{A.10}$$

we obtain (3.1).

B. Two paths ($L = 2$)

Considering the angle estimate of two paths we have

$$\boldsymbol{\theta} = \begin{bmatrix}\alpha_1 & \alpha_2\end{bmatrix}^{\mathrm{T}}. \tag{A.11}$$

Using (A.9), (A.10) and

$${\beta_1}^*\beta_2 = \sqrt{E_{s1}E_{s2}}e^{j\Delta\phi} \tag{A.12}$$

$$\begin{aligned}\mathbf{s}(\tau_1)^{\mathrm{H}}\mathbf{s}(\tau_2) &= \sum_{n=0}^{N-1} s(nT-\tau_1)^* s(nT-\tau_2) \\ &\approx B\int_{-\infty}^{\infty} s(t)^* s(t-\Delta\tau)\mathrm{d}t \\ &= Br(\Delta\tau)\end{aligned} \tag{A.13}$$

we obtain (3.2).

References

[1] W. Ballance and A. Jaffer, "The explicit analytic cramer-rao bound on angle estimation," in *Signals, Systems and Computers, 1988. Twenty-Second Asilomar Conference on*, vol. 1, 1988, pp. 345–351.

[2] P. Stoica and A. Nehorai, "Music, maximum likelihood, and cramer-rao bound," *Acoustics, Speech and Signal Processing, IEEE Transactions on*, vol. 37, no. 5, pp. 720–741, May 1989.

[3] ——, "Music, maximum likelihood, and cramer-rao bound: further results and comparisons," *Acoustics, Speech and Signal Processing, IEEE Transactions on*, vol. 38, no. 12, pp. 2140–2150, Dec 1990.

[4] ——, "Performance study of conditional and unconditional direction-of-arrival estimation," *Acoustics, Speech and Signal Processing, IEEE Transactions on*, vol. 38, no. 10, pp. 1783–1795, Oct 1990.

[5] A. Weiss and B. Friedlander, "On the cramer-rao bound for direction finding of correlated signals," *Signal Processing, IEEE Transactions on*, vol. 41, no. 1, pp. 495–, Jan 1993.

[6] T. Tuncer and B. Friedlander, Eds., *Classical and Modern Direction-of-Arrival Estimation*. Academic Press, 2009.

[7] P. Stoica and R. Moses, *Spectral Analysis of Signals*, T. Robbins, Ed. Prentice Hall, 2005.